

Transcending Lifshitz Theory: Reliable Prediction of Adhesion Forces between Hydrocarbon Surfaces in Condensed Phases using Molecular Contact Thermodynamics

Oscar Siles-Brugge,^{1†} Christopher A Hunter² and Graham J Leggett^{1}*

¹Department of Chemistry, University of Sheffield, Brook Hill, Sheffield S3 7HF, UK and

²Department of Chemistry, University of Cambridge, Lensfield Road, Cambridge CB2 1EW.

ABSTRACT

Works of adhesion W (Lifshitz) between hydrocarbon surfaces in 260 liquids were calculated using Lifshitz theory and compared with interaction free energies $\Delta\Delta G$ determined using a model in which the interactions between a molecule and a liquid are described by a set of surface site interaction points (SSIP). The predictions of these models diverge in significant ways. Interaction free energies calculated using the SSIP approach are typically small and vary little, but in contrast, Lifshitz theory yields works of adhesion that span a broad range. Moreover, the SSIP model also yields significantly different $\Delta\Delta G$ values in some liquids for which, in contrast, Lifshitz theory predicts similar values of W . These divergent predictions were tested using atomic force

microscopy. The experimentally determined work of adhesion was found to be closer to the value predicted using the SSIP model than to $W(\text{Lifshitz})$. Still greater differences were found in the interaction energies calculated using the two models when liquid mixtures were considered. For mixtures of methanol and benzyl alcohol, $\Delta\Delta G$ declines smoothly as the benzyl alcohol concentration increases, but $W(\text{Lifshitz})$ decreases to a minimum and then increases, reaching a larger value for benzyl alcohol than for methanol. The experimental adhesion data were correlated closely with the predictions of the SSIP model. We conclude that the molecular-scale treatment intrinsic to the SSIP approach enables adhesive interactions to be modelled more accurately than is possible using Lifshitz theory, which instead uses the bulk properties of the medium to predict work of adhesion values.

INTRODUCTION

Interfacial interactions regulate a multitude of phenomena,¹ including adhesion,^{2, 3} wetting,⁴⁻⁷ friction⁸ and biological processes⁹ such as protein adsorption,^{10, 11} tissue cell attachment^{10, 12-14} and biofilm formation.^{15, 16} Many techniques have been developed to measure adhesive interactions at surfaces, including the surface forces apparatus,¹⁷⁻¹⁹ the atomic force microscope,^{11, 20-27} contact angle measurement,^{1, 28} peel tests²⁹ and others. To calculate adhesive energies from such measurements, a quantitative model is required that relates the observables (e.g. forces) to the physical properties of the interacting materials (e.g. interfacial free energies). In this paper we compare two different approaches to the determination of interaction energies between solid surfaces in liquids. We contrast the predictions of the Lifshitz model,³⁰⁻³³ in which the interacting surfaces are treated as slabs and the van der Waals force is determined by the mean dielectric properties of the media,¹ with calculations made using a molecular treatment based on functional group interactions between the surfaces and the solvent.³⁴⁻³⁸

There are well-established models for the van der Waals attractive forces between molecules in vacuum. In the gas-phase, pairwise additivity of forces is usually assumed. However, in condensed phases the assumption of pairwise additivity breaks down.¹ The Lifshitz model solves this problem by treating interacting media as continuous phases, and using the mean bulk dielectric properties of interacting phases to calculate the van der Waals forces. The foundations of the Lifshitz model lie in quantum field theory,^{30,31} but subsequently a number of simplifications have been made to broaden its applicability.¹ Lifshitz theory is used to calculate the Hamaker constant A which, together with other terms describing the interacting system, may be used to calculate adhesive forces at interfaces.²⁷ For example, the interaction energy W is given by $W = -AR/6D$ for a hemisphere of radius R interacting with a planar counter-surface at a distance D .¹ This equation provides a realistic model for an atomic force microscope probe, and also for two crossed cylinders with equal radii R , as in the surface forces apparatus.¹

One of us (CAH) has developed an approach to the calculation of non-covalent interaction free energies that is based on the attribution of local interaction parameters to specific sites on molecular surfaces.^{34, 38} These interaction parameters are determined either experimentally or theoretically, and they may be used to calculate the interaction energy and its dependence on the medium. Previously we found that this surface site interaction point (SSIP) model yielded predictions for carboxylic acid terminated surfaces that diverged from those of the Lifshitz model.³⁹ However, it might be argued that this is expected for surfaces containing permanent dipoles that can form directional hydrogen bonds.⁴⁰ In contrast, hydrocarbon surfaces might be expected to behave in greater conformity with the predictions of Lifshitz theory because their interactions are dominated by polarization forces.^{1, 27} However, we here demonstrate that for hydrocarbon surfaces, significant differences are found between interaction energies calculated

using Lifshitz theory and the SSIP model. In this case, the experimental works of adhesion obtained using atomic force microscopy are also predicted more accurately by the SSIP model than by Lifshitz theory.

METHODS

Determination of the work of adhesion using the Lifshitz model

The work of adhesion between identical non-polar surfaces (1) in a liquid medium (3) according to Lifshitz theory was calculated by first determining the Hamaker constant of the system:¹

$$A_H = A_{\nu=0} + A_{\nu>0} \quad (1)$$

where the Hamaker constant (A_H) is the sum of a zero-frequency term $A_{\nu=0}$ due to Keesom (dipole-dipole) and Debye (induced-permanent dipole) interactions, and a non-zero frequency term $A_{\nu>0}$ arising from long-range London dispersion forces. Both of these terms were calculated using the approximate equation derived by Israelachvili.¹ The zero-frequency term is a function of the dielectric constants of the surfaces and liquid medium (ϵ_1 and ϵ_3 , respectively) as:

$$A_{\nu=0} \approx \frac{3}{4} kT \left(\frac{\epsilon_1 - \epsilon_3}{\epsilon_1 + \epsilon_3} \right)^2 \quad (2)$$

where k is the Boltzmann constant ($1.38065 \times 10^{-23} \text{ J K}^{-1}$), T is the absolute temperature (assumed 298.15 K). The non-zero frequency term, determined by the refractive indices of the surfaces and liquid medium (n_1 and n_3 , respectively), is:

$$A_{\nu>0} \approx \frac{3h\nu_e}{16\sqrt{2}} \frac{(n_1^2 - n_3^2)^2}{(n_1^2 + n_3^2)^{3/2}} \quad (3)$$

where h is the Planck constant ($6.62608 \times 10^{-34} \text{ J s}$), and ν_e the main electronic absorption frequency in the UV (assumed $3 \times 10^{15} \text{ s}^{-1}$ for all media). For binary mixtures of methanol and benzyl alcohol, experimentally obtained refractive indices were used, and a linear change in

dielectric constants assumed. From the Hamaker constant, the work of adhesion was calculated using the relation:¹

$$W(\text{Lifshitz}) = \frac{A_H}{12\pi D_0} \quad (4)$$

where D_0 the closest separation between the two surfaces (spherical tip and half-space of the sample). A value of $D_0 = 0.165$ nm has been shown to provide reasonable estimates of the surface energies of various organic materials^{1,41} and was therefore used for this study.

Determination of the interaction free energy $\Delta\Delta G$ using the SSIP model

The free energy of complexation for an equivalent system of interacting surfaces may be obtained from the surface site interaction point (SSIP) model introduced by Hunter.³⁴ The model extends previous work in estimating the solvent effects on equilibrium constants for solute-solute interactions.³⁴ Interactions between a molecule and neighboring molecules in a liquid are described by a set of SSIPs, each of which represents a molecular surface area of 9.5 \AA^2 and volume of 5 \AA^3 . An electrostatic interaction parameter, ε_i , is obtained for each SSIP from the molecular electrostatic potential surface calculated using density functional theory and used to calculate the polar contribution to the interaction between two SSIPs. The non-polar contribution to the interaction between two SSIPs, $E_{\text{VDW}} = -5.6 \text{ kJ mol}^{-1}$, can be treated as a constant, because each SSIP represents the same molecular surface area^{34,42}. The free energy change for the interaction between two solute SSIPs in a liquid is calculated using the SSIMPLE algorithm, which treats the liquid phase as an ensemble of interacting SSIPs at equilibrium. All SSIP interactions are treated in a pairwise manner, such that the association constant for interaction between the i th and j th SSIP, K_{ij} , is given by:

$$K_{ij} = 0.5e^{-E_{ij}/RT} \quad (5)$$

$$E_{ij} = \varepsilon_i \varepsilon_j + E_{vdw} \quad (6)$$

Given the total concentration of each SSIP, Equations 9 and 10 can be used to construct a set of simultaneous equations that can be solved to determine the speciation of SSIP contacts in the liquid. The solvation free energy change for solute 1 is determined from the fraction of free SSIPs (1_f) in the solution:

$$\Delta G_S(1) = RT \ln \left(\frac{[1_f]}{[1]} \right) + \Delta G_c \quad (5)$$

where R is the gas constant ($8.31446 \text{ J K}^{-1} \text{ mol}^{-1}$), T is the standard temperature (298.15 K), and ΔG_c is the confinement free energy that is required to describe phase change equilibria, but in the case will cancel out (see Equations 8 and 9).

The free energy change for the binding of solute 1 into a complex with another solute 2 is described in the same way by treating the complex as a pure phase containing only the solute SSIPs at the same total density as the liquid:

	$\Delta G_b(1) = RT \ln \left(\frac{\sqrt{1 + 4(K_{12} + K_{vdw})\theta} - 1}{2(K_{12} + K_{vdw})\theta} \right) + \Delta G_c$	(8)
--	---	-----

where K_{12} is the association constant for the interaction between solute SSIP 1 and solute SSIP 2 calculated using Equations 5 and 6, K_{vdw} is the corresponding association constant for a non-polar interaction ($E_{ij} = E_{vdw}$), and θ is the total SSIP density of the liquid phase.

The free energy change associated with the exchange of solvent and solute interactions when a complex is formed is given by:

	$\Delta \Delta G = \Delta G_b(1) + \Delta G_b(2) - \Delta G_S(1) - \Delta G_S(2)$	(9)
--	---	-----

To model two interacting non-polar surfaces, the electrostatic interaction parameters for alkanes were used ($\varepsilon_1 = 0.5$ and $\varepsilon_2 = -0.5$) were used to represent the surfaces as two interacting solute SSIPs present at low concentrations relative to the solvent (1 mM). The calculated values of free

energy change were then normalized such that a greater value indicates a greater affinity for the surfaces to form a complex.

Interactions in liquid mixtures

While solvent mixtures are natively possible in the SSIP model, for Lifshitz theory the bulk dielectric constant and refractive index are required. The dielectric constant of a non-polar mixture can be calculated using the Clausius-Mosotti equation⁴³

$$\frac{\varepsilon'_m - 1}{\varepsilon'_m + 2} = \sum_i \frac{4\pi v_i \rho_i N_A \alpha_i}{3M_i} \quad (10)$$

where ε'_m is the dielectric constant of the mixture, N_A is Avogadro's number, and for each component i of the mixture n_i is the volume fraction, r_i is the mass density, a_i is the electric polarizability, and M_i is the molecular weight. The values of these parameters can be obtained from literature. However, it has been found that the dielectric constants of mixtures with one or two non-polar liquids typically display a broadly linear relationship with composition. For mixtures containing two polar liquids, a linear relation between the dielectric constant and the composition was found to yield average deviations of up to 5 % at 298 K. As such, a linear relation was assumed when determining the dielectric constant of the resulting mixtures. For the refractive index, the Lorentz-Lorenz mixing rule was used, as it has been previously shown to yield average deviations of less than 2 % for binary systems of mixtures of several types of liquids:^{44,45}

$$\frac{n_{12}^2 - 1}{n_{12}^2 + 2} = \phi_1 \frac{n_1^2 - 1}{n_1^2 + 2} + \phi_2 \frac{n_2^2 - 1}{n_2^2 + 2} \quad (11)$$

where n_{12} is the refractive index of the mixture, n_1 and n_2 are the refractive indices of the two pure components, and f_1 and f_2 are the volume fractions. For mixtures of benzyl alcohol and methanol, experimentally obtained values for the refractive index of the mixture were used.

EXPERIMENTAL SECTION

Monolayer formation

Self-assembled monolayers were formed using 1-dodecanethiol (DDT, 99%, Sigma Aldrich) as received on gold-coated glass slides (Menzel-Gläser, 22 x 50 mm, #1.5, Braunschweig, Germany). The slides were first cleaned in piranha solution (a mixture of concentrated sulfuric acid and hydrogen peroxide with a 70:30 volume ratio; **Caution! Piranha solution is a strong oxidizing agent and can detonate unexpectedly on contact with organic materials**) and rinsed thoroughly in deionized water (Veolia Water Technologies, High Wycombe, UK). The slides were then immersed in RCA solution ($\text{H}_2\text{O}_2/\text{NH}_3/\text{H}_2\text{O}$, 1:2:5 volume ratio) for 30 min and rinsed thoroughly in deionized water after cooling. The slides were allowed to dry for at least 2 h in a clean 120°C oven before metal evaporation.

AFM probe preparation

Commercial V-shaped silicon nitride AFM probes (DNP-10, Bruker AFM Probes) with a nominal spring constant of 0.12 N m^{-1} were used for force spectroscopy and friction force measurements. Previous studies have shown that these commercially available AFM probes, usually supplied in protective gel packs, have high levels of polydimethylsiloxane (PDMS) contamination. Due to damage observed in the AFM probes after piranha cleaning (the reflective layer is often damaged), the probes were cleaned using a ProCleaner Plus UV/Ozone cleaner (BioForce, Salt Lake City, USA) for 30 min. After exposure to ozone, the probes were rinsed in HPLC-grade ethanol and gently dried in a stream of N_2 . Probes and slides for DDT SAM formation were coated with a 1 nm chromium (Cr, 99.5%, Sigma Aldrich) adhesive layer at a rate of 0.01 nm s^{-1} , followed by a 10 nm layer of gold (Au, 99.999%, Goodfellow metals) deposited at 0.03

nm s⁻¹ in an Edwards Auto 306 thermal evaporator with bell jar and diffusion pump at operating pressures of 10⁻⁶ mbar.

SAM-functionalized probes were prepared by immersion of gold-coated probes in a 1mM solution of DDT in degassed HPLC-grade ethanol for 24 h. Probes washed with copious amounts of HPLC-grade ethanol and dried in a stream of N₂ before use.

Atomic force microscopy

n-Heptane (HPLC, Fisher Scientific), water (18 MΩ), ethanol (HPLC, Fisher Scientific), methanol (anhydrous, 99.8%, Sigma Aldrich), benzyl alcohol (anhydrous, 99.8%, Sigma Aldrich), benzonitrile (anhydrous, ≥ 99%, Sigma Aldrich), 1,2,4-trichlorobenzene (anhydrous, ≥ 99%, Sigma Aldrich) were all used as received and injected into the AFM fluid cell using a piranha-cleaned glass syringe.

All measurements were made on a NanoScope V MultiMode 8 (Bruker UK Ltd, Coventry, UK) in conjunction with a J-scanner. Calibration of the lateral and normal forces was performed in two stages. The normal spring constant was calibrated at the beginning of all experimental procedures for any given probe using the thermal noise technique first described by Hutter and Bechhoefer, implemented *via* the calibration routine in the microscope operating system, with a correction factor of 0.93 for V-shaped AFM probes.

To calibrate lateral forces, the wedge calibration method introduced by Ogletree *et al* and adapted to include adhesion by Varenberg *et al* was used. To facilitate probe calibration, friction measurements across a flat and inclined surface were required. A commercially available silicon calibration grating (TGF11, Mikromasch, Sofia, Bulgaria) was used for this purpose, and all images were obtained in ethanol. Tip radii were determined by imaging a commercially available

silicon calibration grating (TGG01, Mikromasch) at 0° and 90° scan angles. The geometric mean radius of the tip was determined by the Zenhausern model of deconvolution.

Force curves were obtained at 300 locations on each sample, repeated across three different samples and probes in each liquid. Following the algorithm used in Carpick's Toolbox, the pull-off forces were calculated from the difference between the load and unload curves at the point of contact. Friction-load plots were obtained by decreasing the applied load from ca. 10 nN until tip-sample separation occurred in 0.7 nN decrements, recording a $1 \times 0.0625 \mu\text{m}^2$ friction image at each load. This process was repeated a minimum of 10 times per liquid at different locations. The average trace-minus-retrace (TMR) friction signal at each line was halved, and then averaged across all collected lines for each applied load.

RESULTS AND DISCUSSION

Interaction Energies in Pure Liquids

The work of adhesion $W(\text{Lifshitz})$ between two hydrocarbon surfaces in a liquid medium was calculated for 260 different liquids using Lifshitz theory (see Supplementary Information for a full list of the liquids modelled). Self-assembled monolayers (SAMs) of dodecanethiol (DDT) were selected as model hydrocarbon surfaces for these calculations. Values of $W(\text{Lifshitz})$ span more than 4 orders of magnitude, from $6 \times 10^{-4} \text{ mJ m}^{-2}$ in tetramethyl silane to 25.7 mJ m^{-2} in dibutyl sulfoxide.

The interaction free energy $\Delta\Delta G$ was calculated for the same systems using the SSIP model. In this case, the calculated values span only two orders of magnitude, from 0.04 kJ mol^{-1} in tetramethyl silane to 4.2 kJ mol^{-1} in sulfur dioxide.

The value of $\Delta\Delta G$ is plotted as a function of $W(\text{Lifshitz})$ in Figure 1. It is striking that a large group of liquids with very different $W(\text{Lifshitz})$ values yields $\Delta\Delta G$ values ≤ 0.5 kJ mol⁻¹. Moreover, there are also liquids that yield similar works of adhesion but very different $\Delta\Delta G$ values. For example, the values of $W(\text{Lifshitz})$ in benzyl alcohol, methanol and water are 5.31 (red square in Figure 1), 4.95 (blue circle) and 4.98 (green diamond) mJ m⁻² respectively, but the interaction free energies in the three liquids are calculated to be 0.36, 0.80 and 4.17 kJ mol⁻¹, respectively. Thus, for three liquids with very similar $W(\text{Lifshitz})$ values, the smallest and largest interaction free energies differ by an order of magnitude.

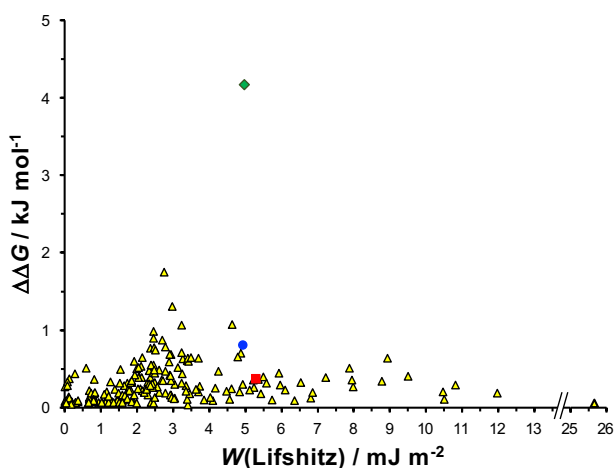


Figure 1. Interaction free energies $\Delta\Delta G$ calculated using the SSIP model as a function of the work of adhesion $W(\text{Lifshitz})$ calculated using Lifshitz theory for 260 different liquids. Values are highlighted for benzyl alcohol (red square), methanol (blue circle) and water (green diamond).

We conclude from the data in Figure 1 that Lifshitz theory and the SSIP model yield divergent predictions for many liquids. To examine further the predictions of these two models, data are plotted in Figure 2 for series of alkanes and for aliphatic polar liquids organized according to functional group.

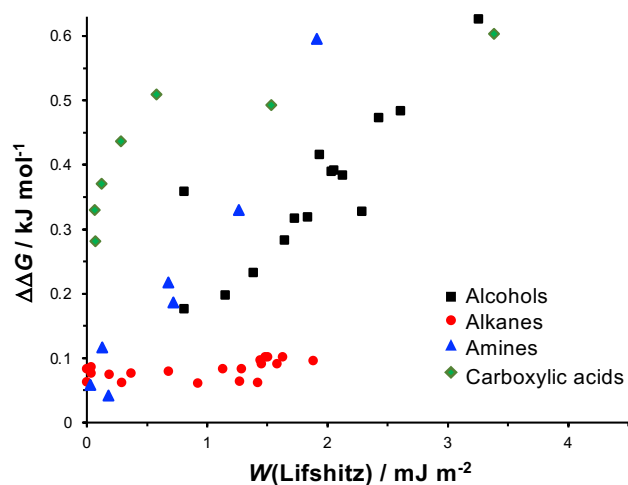


Figure 2. Relationship between the interaction free energy $\Delta\Delta G$ calculated using the SSIP model and the Lifshitz work of adhesion $W(\text{Lifshitz})$ for hydrocarbon surfaces interacting in series of alkanes and polar liquids.

The most marked difference between the predictions of the two models is observed for the alkanes (red circles), for which the SSIP model yields values of $\Delta\Delta G$ that are almost invariant with $W(\text{Lifshitz})$. Large deviations are also observed between the predictions of the two models for carboxylic acids. For a number of carboxylic acids with $W(\text{Lifshitz}) < 0.5 \text{ mJ m}^{-2}$, $\Delta\Delta G$ increases significantly for comparatively small changes in $W(\text{Lifshitz})$, but a limiting value of $\Delta\Delta G$ is reached for $W(\text{Lifshitz}) > 0.5 \text{ mJ m}^{-2}$.

More subtle differences are observed for alcohols and amines. For both these series of liquids, the interaction free energy is proportional to the work of adhesion. However, the constant of proportionality is clearly different for these two series of liquids, indicating that there is divergence between the predictions of the two models. The work of adhesion can be estimated from the $\Delta\Delta G$ data by using the relationship $W(\text{SSIP}) \sim \Delta\Delta G/\sigma$, where σ is the area occupied by an adsorbate in a DDT SAM.⁴⁶ Thus, we estimate that $W(\text{SSIP}) \sim 5/2 W(\text{Lifshitz})$ for amines, representing a substantial difference between the predictions of the two models.

Table 1. Relative permittivities (ϵ), refractive indices (n_D , measured at sodium D line), adhesion forces F_{po} and works of adhesion $W(\text{exp})$ determined from AFM measurements, and works of adhesion calculated using the Lifshitz ($W(\text{Lifshitz})$) and SSIP models ($W(\text{SSIP})$) for DDT SAMs interacting in a range of pure liquids. Bulk values for dodecanethiol are included for reference. ϵ , n_D average values at 20°C obtained from Marcus et al.⁴⁷ and Lide et al.⁴⁸

Liquid	n_D	ϵ	F_{po}/R / mN m ⁻¹	$W(\text{exp})$ / mJ m ⁻²	$W(\text{Lifshitz})$ / mJ m ⁻²	$W(\text{SSIP})$ / mJ m ⁻²
dodecanethiol	1.420	2.00	–	–	–	–
water	1.333	78.36	292 ± 12	46.5 ± 1.9	4.98	37.08
methanol	1.327	32.66	41 ± 4	6.52 ± 0.53	4.95	7.19
ethanol	1.359	24.55	34 ± 4	5.41 ± 0.63	3.26	5.61
nitromethane	1.379	35.87	30 ± 3	4.77 ± 0.51	2.91	3.80
benzyl alcohol	1.538	12.70	8.3 ± 2.1	1.32 ± 0.33	5.31	3.28
benzonitrile	1.525	25.20	4.2 ± 1.6	0.67 ± 0.25	5.11	2.03
<i>n</i> -heptane	1.385	1.92	2.8 ± 1.0	0.45 ± 0.16	0.39	0.72
<i>n</i> -decane	1.410	1.99	3.8 ± 1.1	0.60 ± 0.18	0.04	0.73
<i>n</i> -dodecane	1.420	2.00	2.4 ± 0.9	0.38 ± 0.14	0.00	0.78
<i>n</i> -hexadecane	1.433	2.05	1.7 ± 1.0	0.27 ± 0.16	0.04	0.81
1,2,4-trichloro- benzene	1.571	4.15	2.7 ± 1.4	0.43 ± 0.22	6.36	0.81

To test the interaction energies calculated using the Lifshitz and SSIP models against experimental data, measurements of pull-off forces were made by AFM for DDT SAMs interacting in a representative selection of pure liquids that included both aliphatic and aromatic solvents and polar and non-polar liquids. A silicon nitride probe was coated with a thin layer of gold, and a self-

assembled monolayer of dodecanthiol (DDT) was formed by immersion of the probe in a dilute solution of the thiol in ethanol. A counter-surface was prepared by forming a DDT SAM on a continuous polycrystalline gold film supported on a glass substrate, and the tip-sample adhesion force F_{po} was measured. Values of F_{po} are shown in Table 1 for an illustrative selection of liquids with varying dielectric constants. It is important to note that measurements by AFM are constrained by both the physical properties of the liquids (liquids with very small surface tensions are difficult to handle in the AFM liquid cell) and also the associated hazards (evaporation occurs from the liquid cell and the risk of exposure to vapor need to be considered carefully).

To enable comparison of these experimental data with predictions made using the Lifshitz and SSIP models, the experimental work of adhesion was calculated from the F_{po} values. If the tip-sample contact is described using the Derjaguin-Muller-Toporov (DMT) model of contact mechanics, the pull-off force is related to the experimental work of adhesion $W(\text{exp})$ by¹

$$F_{po} = 2\pi RW(\text{exp}) \quad (12)$$

The resulting experimental works of adhesion are displayed in Table 1 together with calculated values determined using the Lifshitz and SSIP models. The Lifshitz works of adhesion are those plotted in Figure 1 and tabulated in the Supporting Information. The SSIP work of adhesion was estimated using the relationship $W(\text{SSIP}) \sim \Delta\Delta G/\sigma$.

The most striking difference between the two models is observed in water. The Lifshitz work of adhesion for DDT SAMs in this liquid, 4.98 mJ m^{-2} , is nearly an order of magnitude smaller than the experimental value, $46.5 \pm 1.9 \text{ mJ m}^{-2}$. In contrast, the value of $W(\text{SSIP})$, 37.08 mJ m^{-2} , is close to the experimental work of adhesion.

For methanol, the Lifshitz work of adhesion, 4.95 mJ m^{-2} , is similar to the value calculated in water, whereas $W(\text{SSIP})$, 7.19 mJ m^{-2} , is much closer to the experimental value of $6.52 \pm 0.53 \text{ mJ}$

m^{-2} . For ethanol, both models correctly yield a work of adhesion that is smaller than that in methanol, but again, the $W(\text{SSIP})$ value, 5.61 mJ m^{-2} , is much closer to the experimentally-determined value, $5.41 \pm 0.63 \text{ mJ m}^{-2}$, than $W(\text{Lifshitz})$, 3.26 mJ m^{-2} .

Both models over-estimate the work of adhesion in the aromatic liquids, benzyl alcohol and benzonitrile. However, the SSIP model yields values that are closest to the experimental data in both liquids, and correctly predicts that the work of adhesion will be substantially larger in benzyl alcohol than in benzonitrile, whereas the Lifshitz model incorrectly yields very similar works of adhesion for these two liquids.

For the remaining five liquids, the Lifshitz model yields values that span two orders of magnitude, from 0.00 mJ m^{-2} for *n*-dodecane and 0.04 mJ m^{-2} for *n*-decane and *n*-hexadecane, to 0.39 mJ m^{-2} for *n*-heptane and 6.36 mJ m^{-2} for 1,2,4-trichloro-benzene. In sharp contrast, the SSIP model yields values that range from 0.72 mJ m^{-2} for *n*-heptane to 0.81 mJ m^{-2} for 1,2,4-trichloro-benzene. The experimental works of adhesion span a slightly larger range, from $0.27 \pm 0.16 \text{ mJ m}^{-2}$ to $0.60 \pm 0.18 \text{ mJ m}^{-2}$ but bearing in mind the experimental uncertainty, the behaviour is broadly consistent with the predictions of the SSIP model; certainly, these data do not display the orders-of-magnitude changes predicted by the Lifshitz model.

Figure 3 shows the experimental work of adhesion data from Table 1 $W(\text{exp})$ as a function of $W(\text{SSIP})$ and $W(\text{Lifshitz})$. While the value of W_{exp} increases with $W(\text{SSIP})$ (a regression coefficient of 0.84 is obtained for the straight line fit in Fig 3a), there is no correlation between the value of $W(\text{Lifshitz})$ and $W(\text{exp})$ in Fig 3b.

In summary, works of adhesion determined experimentally from AFM adhesion force measurements are correlated closely with interaction free energies calculated using the SSIP

model. In contrast, works of adhesion calculated using the Lifshitz model are not well correlated with the experimental data.

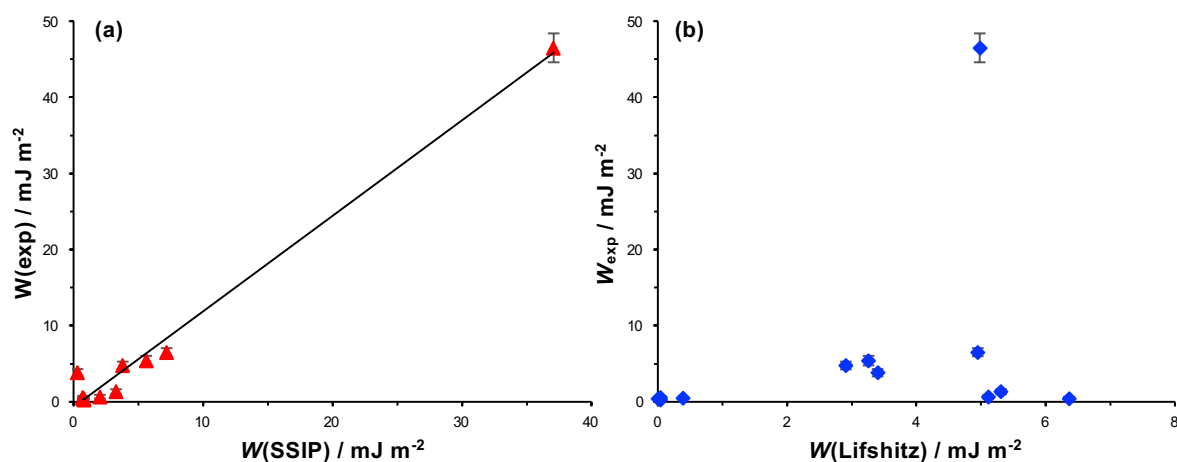


Figure 3. Experimental work of adhesion data from Table 1 displayed as a function of (a) the work of adhesion calculated using the SSIP model and (b) the Lifshitz work of adhesion.

Methanol and Benzyl Alcohol: Nanotribological Measurements

Using the Lifshitz model, we calculated that the work of adhesion for interacting DDT SAMs is slightly larger (5.31 mJ m^{-2}) in pure benzyl alcohol than in pure methanol (4.95 mJ m^{-2}). In contrast, using the SSIP model, we calculated interaction energies of 3.28 mJ m^{-2} and 7.19 mJ m^{-2} , respectively. Thus, the two models yield significantly different predictions for these pure liquids. Histograms of pull-off forces F_{po} are shown in Figure 4a. In benzyl alcohol (red triangles), the pull-off force peaks at small values, and the distribution of forces is narrow. However, in methanol, the distribution of forces is broader and the maximum in the frequency distribution lies between 2.1 and 2.4 nN, indicating a significantly stronger adhesion force in this liquid, consistent with the predictions of the SSIP model and contrary to the predictions of the Lifshitz model.

Friction-load relationships were acquired for DDT-functionalized AFM probes in contact with DDT SAMs. Following the work of Bowden and Tabor, Carpick and others, we treat the friction

force F_F in the sliding contact as the sum of two terms, an area-dependent shear term characterized by a surface shear strength τ and a load-dependent term attributed to "molecular ploughing" characterized by a coefficient of friction μ :

$$F_F = \mu(F_N + F_a) + \pi \left(\frac{R}{K}\right)^{\frac{2}{3}} \tau (F_N + F_a)^{\frac{2}{3}} \quad (13)$$

where F_N is the load perpendicular to the planar counter-surface, F_a is the adhesion force, R is the radius of the probe and K is the elastic modulus of the materials in contact. In studies of a variety of materials, including self-assembled monolayers and surface-grafted polymers, we showed that for solvated interfaces the work of adhesion is typically small, and sliding is dominated by molecular ploughing; thus, the shear term becomes small and the friction-load relationship is linear. In this regime, energy dissipation is largely through the deformation of molecules under the probe (e.g. through the creation of gauche defects in SAMs). However, as the interface becomes increasingly less well solvated, the shear term begins to make an important contribution to friction; energy is increasingly dissipated in shearing and the friction-load relationship becomes non-linear. Thus, in general a linear friction-load relationship indicates weak adhesion (dissipation dominated by ploughing) and a non-linear friction-load relationship indicates strong adhesion (dissipation dominated by shearing).

Figure 4b shows friction-load relationships acquired for DDT contacts in methanol and benzyl alcohol. It is clear that while the friction-load relationship is linear in benzyl alcohol, with a coefficient of friction $\mu = 0.11 \pm 0.02$, it is non-linear in methanol. While the shear term is negligible after fitting friction-load data measured in benzyl alcohol, it is the load-dependent term that is negligible in methanol, and fitting of the curve yields a surface shear strength $\tau/K^{2/3} = 2.17 \pm 0.43 \text{ Pa}^{1/3}$. This indicates that in benzyl alcohol the main dissipative pathway is via ploughing

(correlated with weak adhesion) whereas in methanol shearing dominates, consistent with strong adhesion. This qualitative difference in the nature of the friction-load relationship is consistent with the predictions of the SSIP model, and refutes the prediction based on the Lifshitz model that adhesion is similar for contacts in methanol and benzyl alcohol.

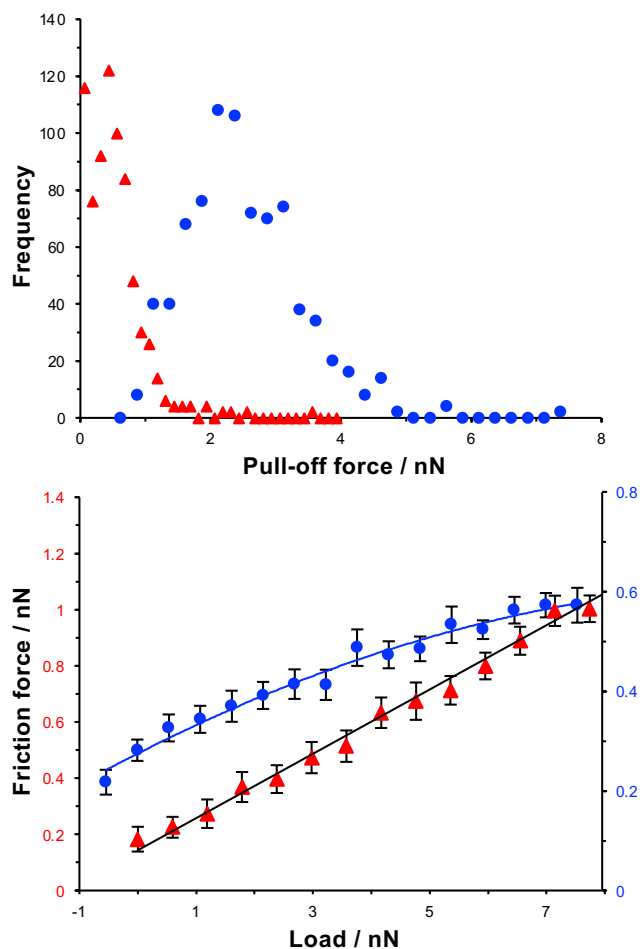


Figure 4. Pull-off force frequency distributions (a) and friction-load relationships (b) for DDT SAMs interacting in benzyl alcohol (red triangles) and methanol (blue circles). Lines in (b) are fitted using equation (13).

Interaction Energies in Mixtures of Methanol and Benzyl Alcohol

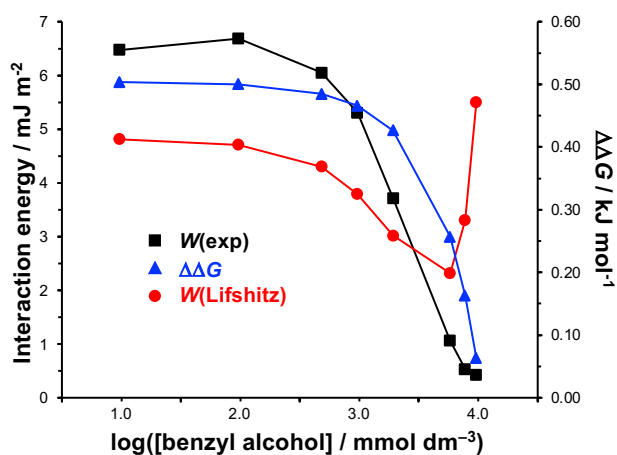


Figure 5. Interaction energies determined experimentally from AFM force measurements (black squares) and by calculation using the Lifshitz (red circles) and SSIP (blue triangles) models for mixtures of benzyl alcohol and methanol, with mole fractions of benzyl alcohol ranging from 0.01 to 1.0.

To test further the predictive capabilities of the Lifshitz and SSIP models, we calculated interaction energies for hydrocarbon surfaces in mixtures of methanol and benzyl alcohol. Data are shown in Fig 5. The concentration of benzyl alcohol is shown on the horizontal axis. In the SSIP model (blue triangles), as $\log([\text{benzyl alcohol}] / \text{mmol dm}^{-3})$ increases from 1 to 2.5, the interaction free energy changes comparatively little. However, as $\log([\text{benzyl alcohol}] / \text{mmol dm}^{-3})$ is increased above 2.5, the interaction free energy begins to decrease, and falls steeply from 3.8 to 4.0. This behavior can be understood in terms of the solvent-surface interaction: methanol interacts weakly with the hydrocarbon surfaces, and only perturbs the adhesive interaction in a small way; in contrast, benzyl alcohol interacts more strongly with the DDT SAMs, coordinating to them more extensively and shifting the equilibrium in the direction of a solvated interface, thus

reducing the strength of adhesion between the probe and counter-surface when they interact. Works of adhesion were also calculated using the Lifshitz model (red circles). Between $\log([\text{benzyl alcohol}] / \text{mmol dm}^{-3})$ of 1 and 2.5, the work of adhesion decreases slowly, but at higher concentrations of benzyl alcohol the work of adhesion begins to decrease more rapidly, mirroring the behavior of the SSIP model. However, in contrast to the SSIP model, a minimum is reached between $\log([\text{benzyl alcohol}] / \text{mmol dm}^{-3}) = 3.3$ and 3.8, and at higher benzyl alcohol concentrations the work of adhesion increases sharply, reaching a value at $\log([\text{benzyl alcohol}] / \text{mmol dm}^{-3}) = 4.0$ that is larger than the value obtained at the lowest benzyl alcohol concentration.

Figure 5 shows experimental work of adhesion data acquired by AFM, using the previously described methodology (black squares). These data match the trend predicted by the SSIP model, although the experimental work of adhesion $W(\text{exp})$ decreases in magnitude slightly more quickly as the concentration of benzyl alcohol is increased. The value of W_{exp} reaches a minimum in pure benzyl alcohol, as predicted by the SSIP model and in contrast to the Lifshitz model, which predicts a maximum value in this liquid. Thus, we conclude that for mixtures of benzyl alcohol and methanol, the experimental data are predicted significantly more reliably by the SSIP model than by the Lifshitz model.

These data further support the hypothesis that works of adhesion determined experimentally from AFM adhesion force measurements are correlated more closely with interaction free energies calculated using the SSIP model than with works of adhesion calculated using the Lifshitz model.

CONCLUSIONS

We calculated interaction energies for hydrocarbon surfaces in 260 liquids using Isrealchvilli's modified form of the Lifshitz theory and Hunter's surface site interaction point (SSIP) model. Values of the work of adhesion calculated using Lifshitz theory spanned a wide range, from 6 x

10^{-4} mJ m⁻² in tetramethyl silane to 25.7 mJ m⁻² in dibutyl sulfoxide. However, the SSIP model predicts much smaller differences in the interaction free energy for the majority of these liquids. When these predictions are compared with measurements made using AFM, the SSIP approach is found to yield works of adhesion that are significantly closer to the experimental data than the predictions made using the Lifshitz model. For some liquids for which Lifshitz theory predicts similar works of adhesion, the SSIP model predicts very different values. In these cases, the experimental data are consistent with the predictions of the SSIP model and are not correlated with the predictions made using the Lifshitz model. For methanol, dissipation in sliding contacts between hydrocarbon monolayers is dominated by shearing, while in benzyl alcohol, dissipation is through molecular ploughing. These differences are consistent with the large difference in work of adhesion predicted using the SSIP model, and with measurements of adhesion forces, while in contrast the Lifshitz model predicts that the works of adhesion measured in these two liquids are very similar. In methanol/benzyl alcohol mixtures, works of adhesion calculated using the Lifshitz model pass through a minimum and approach a maximum in pure benzyl alcohol, whereas experimental pull-off force values and works of adhesion calculated using the SSIP model decline to reach a minimum in pure benzyl alcohol. We conclude that the use of mean bulk dielectric properties to calculate interaction energies using the Lifshitz model represents a significant and under-appreciated limitation. A molecular approach based upon a thermodynamic analysis of interfacial equilibria using the SSIP model yields predictions that are more reliable and much closer experimental data.

ASSOCIATED CONTENT

Supporting Information. Dielectric constants, refractive indices, Lifshitz works of adhesion and interaction free energies for dodecanethiol SAMs in 260 liquids.

AUTHOR INFORMATION

Corresponding Author

*E-mail: Graham.Leggett@sheffield.ac.uk

Present Addresses

†Present address: Department of Chemistry, University of Nottingham, University Park,
Nottingham NG7 2RD.

ACKNOWLEDGMENT

OSB thanks the EPSRC Centre for Doctoral Training in Molecular-Scale Engineering (EP/J500124/1) for a research studentship.

REFERENCES

- (1) Israelachvili, J. N. *Intermolecular and Surface Forces*; Academic Press, 1992.
- (2) Kendall, K. Adhesion: Molecules and mechanics. *Science* **1994**, *263*, 1720-1725.
- (3) Creton, C.; Ciccotti, M. Fracture and adhesion of soft materials: a review. *Rep. Prog. Phys.* **2016**, *79*, 046601
- (4) Mohammed, M.; Babadagli, T. Wettability alteration: A comprehensive review of materials/methods and testing the selected ones on heavy-oil containing oil-wet systems. *Adv. Coll. Interface Sci.* **2015**, *220*, 54-77.

- (5) Li, S.; Huang, J.; Chen, Z.; Chen, G.; Lai, Y. A review on special wettability textiles: theoretical models, fabrication technologies and multifunctional applications. *J. Mater. Chem. A* **2017**, *5*, 31-55.
- (6) Feng, J.; Guo, Z. Wettability of graphene: from influencing factors and reversible conversions to potential applications. *Nanoscale Horiz.* **2019**, *4*, 339-364.
- (7) Andreotti, B.; Snoeijer, J. H. Statics and dynamics of soft wetting. *Ann. Rev. Fluid Mech.* **2020**, *52*, 285-308.
- (8) Park, J. Y.; Salmeron, M. Fundamental aspects of energy dissipation in friction. *Chem. Rev.* **2014**, *114*, 677-711.
- (9) Marshall, S. J.; Bayne, S. C.; Baier, R.; Tomsia, A. P.; Marshall, G. W. A review of adhesion science. *Dent. Mater.* **2010**, *26*, e11-e16.
- (10) Frutiger, A.; Tanno, A.; Hwu, S.; Tiefenauer, R. F.; Vörös, J.; Nakatsuka, N. Nonspecific binding—fundamental concepts and consequences for biosensing applications. *Chem. Rev.* **2021**, *121*, 8095-8160.
- (11) Feldman, K.; Haehner, G.; Spencer, N. D.; Harder, P.; Grunze, M. Probing resistance to protein adsorption of oligo(ethylene glycol)-terminated self-assembled monolayers by scanning force microscopy. *J. Am. Chem. Soc.* **1999**, *121*, 10134-10141.
- (12) Bouten, P. J. M.; Zonjee, M.; Bender, J.; Yauw, S. T. K.; van Goor, H.; van Hest, J. C. M.; Hoogenboom, R. The chemistry of tissue adhesive materials. *Prog. Polym. Sci.* **2014**, *39*, 1375-1405.

- (13) Dubiel, E. A.; Martin, Y.; Vermette, P. Bridging the gap between physicochemistry and interpretation prevalent in cell–surface interactions. *Chem. Rev.* **2011**, *111*, 2900-2936.
- (14) Nam, S.; Mooney, D. Polymeric tissue adhesives. *Chem. Rev.* **2021**, *121*, 11336-11384.
- (15) Waite, J. H. Mussel adhesion – essential footwork. *J. Exp. Biol.* **2017**, *220*, 517-530.
- (16) Beaussart, A.; Feuillie, C.; El-Kirat-Chatel, S. The microbial adhesive arsenal deciphered by atomic force microscopy. *Nanoscale* **2020**, *12*, 23885-23896.
- (17) Tabor, D.; Winterton, R. H. S. The direct measurement of normal and retarded van der Waals Forces. *Proc. Roy. Soc. A* **1969**, *312*, 435–450.
- (18) Israelachvili, J. N.; Adams, G. E. Direct measurement of long range forces between two mica surfaces in aqueous KNO₃ solutions. *Nature* **1976**, *262*, 774–776.
- (19) Israelachvili, J. N.; Min, Y.; Akbulut, M.; Alig, A.; Carver, G.; Greene, W.; Kristiansen, K.; Meyer, E.; Pesika, N. Recent advances in the surface forces apparatus (SFA) technique. *Rep. Prog. Phys.* **2010**, *73*, 036601.
- (20) Binnig, G.; Quate, C. F.; Gerber, C. Atomic force microscope. *Phys. Rev. Lett.* **1986**, *56*, 930-933.
- (21) Giessibl, F. J. Advances in atomic force microscopy. *Rev. Mod. Phys.* **2003**, *75*, 949-983.
- (22) Nguyen-Tri, P.; Ghassemi, P.; Carriere, P.; Nanda, S.; Assadi, A. A.; Nguyen, D. D. Recent applications of advanced atomic force microscopy in polymer science: a review. *Polymers* **2020**, *12*, 1142-1169.

(23) Sedin, D. L.; Rowlen, K. L. Adhesion forces measured by atomic force microscopy in humid air. *Anal. Chem.* **2000**, *72*, 2183-2189.

(24) Jiang, Y.; Turner, K. T. Measurement of the strength and range of adhesion using atomic force microscopy. *Extreme Mech. Lett.* **2016**, *9*, 119-126.

(25) Jiang, T.; Zhu, Y. Measuring graphene adhesion using atomic force microscopy with a microsphere tip. *Nanoscale* **2015**, *7*, 10760-10766.

(26) Leite, F. L.; Bueno, C. C.; Róz, A. L. D.; Ziemath, E. C.; Jr, O. N. O. Theoretical models for surface forces and adhesion and their measurement using atomic force microscopy. *Int. J. Mol. Sci.* **2012**, *13*, 12773-12856.

(27) Feldman, K.; Tervoort, T.; Smith, P.; Spencer, N. D. Toward a force spectroscopy of polymer surfaces. *Langmuir* **1998**, *14*, 372-378.

(28) Adamson, A. W.; Gast, A. P. *Physical Chemistry of Surfaces*; Wiley, 1997.

(29) Bartlett, M. D.; Case, S. W.; Kinloch, A. J.; Dillard, D. A. Peel tests for quantifying adhesion and toughness: a review. *Prog. Mater. Sci.* **2023**, *137*, 101086.

(30) Lifshitz, E. M. The theory of molecular attractive forces between solids. *J. Exp. Theor. Phys. USSR* **1954**, *29*, 94-110.

(31) Lifshitz, E. M. The theory of molecular attractive forces between solids. *Sov. Phys.* **1956**, *2*, 73-83.

(32) Derjaguin, B. V.; Abrikosova, I. I.; Lifshitz, E. M. Direct measurement of molecular attraction between solids separated by a narrow gap. *Quart. Rev. Chem. Soc.* **1956**, *10*, 295-329.

- (33) Israelachvili, J. N.; Tabor, D. Van der Waals Forces: theory and experiment. *Prog. Surf. Membrane Sci.* **1973**, *7*, 1–55.
- (34) Hunter, C. A. Quantifying intermolecular interactions: guidelines for the molecular recognition toolbox. *Angew. Chem. Int. Ed.* **2004**, *43*, 5310-5324.
- (35) Robertson, C. C.; Wright, J. S.; Carrington, E. J.; Perutz, R. N.; Hunter, C. A.; Brammer, L. Hydrogen bonding vs. halogen bonding: the solvent decides. *Chem. Sci.* **2017**, *8*, 5392-5398.
- (36) Driver, M. D.; Williamson, M. J.; Cook, Joanne L.; Hunter, C. A. Functional group interaction profiles: a general treatment of solvent effects on non-covalent interactions. *Chem. Sci.* **2020**, *11*, 4456-4466.
- (37) Reynolds, D. P.; Storer, M. C.; Hunter, C. A. An empirical model for solvation based on surface site interaction points. *Chem. Sci.* **2021**, *12*, 13193-13208.
- (38) Storer, M. C.; Hunter, C. A. The surface site interaction point approach to non-covalent interactions. *Chem. Soc. Rev.* **2022**, *51*, 10064-10082.
- (39) Busuttill, K.; Geoghegan, M.; Hunter, C. A.; Leggett, G. J. Contact mechanics of nanometer-scale molecular contacts: correlation between adhesion, friction, and hydrogen bond thermodynamics. *J. Am. Chem. Soc.* **2011**, *133*, 8625-8632.
- (40) Nikogeorgos, N.; Hunter, C. A.; Leggett, G. J. Relationship between molecular contact thermodynamics and surface contact mechanics. *Langmuir* **2012**, *28*, 17709-17717.
- (41) Mate, C. M. *Tribology on the small scale*; Oxford University Press, 2008.
- (42) Hunter, C. A. van der Waals interactions in non-polar liquids. *Chem. Sci.* **2013**, *4*, 834-848.

- (43) Hill, N. *Dielectric properties and molecular behaviour*; Van Nostrand Reinhold.
- (44) Mehra, R. Application of refractive index mixing rules in binary systems of hexadecane and heptadecane with n-alkanols at different temperatures. *J. Chem. Sci.* **2003**, *115*, 147-154.
- (45) Tasic, A. Z.; Djordjevic, B. D.; Grozdanic, D. K.; Radojkovic, N. *J. Chem. Eng. Data* **1992**, *37*, 310-313.
- (46) Love, J. C.; Estroff, L. A.; Kriebel, J. K.; Nuzzo, R. G.; Whitesides, G. M. Self-Assembled Monolayers of Thiolates on Metals as a Form of Nanotechnology. *Chem. Rev.* **2005**, *105*, 1103-1170.
- (47) Marcus, Y. In *The properties of solvents*, Wiley, 1998; pp 95–102.
- (48) Lide, D. R. *CRC Handbook of Chemistry and Physics*; Taylor & Francis, 2003.

SYNOPSIS

